

Convolution-Smoothing Based Locally Sparse Estimation for Functional Quantile Regression

Hua Liu^{*a}, Boyi Hu^{* b}, Jinhong You^c, and Jiguo Cao^{†d}

^aSchool of Economics and Finance, Xi'an Jiaotong University

^bDepartment of Neurology, College of Physicians and Surgeons, Columbia University

^cSchool of Statistics and Data Science, Shanghai University of Finance and Economics

^dDepartment of Statistics and Actuarial Science, Simon Fraser University

Convolution-Smoothing based Locally Sparse Estimation for Functional Quantile Regression

Abstract

Motivated by an application to study the impact of temperature, precipitation and irrigation on soybean yield, this article proposes a sparse semi-parametric functional quantile model. The model is called sparse because the functional coefficients are only nonzero in the local time region where the functional covariates have significant effects on the response under different quantile levels. To tackle the computational and theoretical challenges in optimizing the quantile loss function added with a concave penalty, we develop a novel Convolution-smoothing based Locally Sparse Estimation (CLOSE) method, to do three tasks in one step, including selecting significant functional covariates, identifying the nonzero region of functional coefficients to enhance the interpretability of the model and estimating the functional coefficients. We establish the functional oracle properties and simultaneous confidence bands for the estimated functional coefficients, along with the asymptotic normality for the estimated parameters. In addition, because it is difficult to estimate the conditional density function given the scalar and functional covariates, we propose the split wild bootstrap method to construct the confidence interval of the estimated parameters and simultaneous confidence band for the functional coefficients. We also establish

^{*}These two authors contributed equally to this paper and shared the first authorship.

[†]Corresponding Author. Email: jiguo_cao@sfu.ca

the consistency of the split wild bootstrap method. The finite sample performance of the proposed CLoSE method is assessed with simulation studies. The proposed model and estimation procedure are also illustrated by identifying the active time regions when the daily temperature influences the soybean yield.

Keywords: Functional data analysis, Functional oracle property, Semi-parametric model

1 Introduction

In agriculture, crop yield is a key focus worldwide because of its direct connection to the global needs for food, feed, and fuel. In addition, crops are highly liquid in the futures market, so crop price fluctuations can directly affect the stability of financial markets. As one of the most important crops worldwide, more than three-quarters of soybeans are used to feed livestock, and only a small percentage (about 7%) of global soybeans are used for typical soybean products such as tofu and soy milk. Meanwhile, the growing appetite for meat, dairy and soybean oil results in a rapidly increasing demand for soybeans as shown in Figure 1-(a). There are two main ways to increase production: to expand the amount of land to grow soybeans and to improve soybean yields (increasing per area harvest). Taking data from the United States as an example, it is clear that the impressive improvement in soybean yields (Figure 1-(b)) is not able to keep up with the increasing demand for soybean production (Figure 1-(c)), which makes the government have to devote additional land to production. However, many scientists think increasing harvested area is a major underlying cause of deforestation. Therefore, it is urgent to improve soybean yields due to increasing product demand and environmental protection.

It is widely known that soybean is a crop with high demands on the natural environment and resources, especially in temperature and humidity. For example, Szczerba et al. (2021) investigated the effects of temperature on germination and seedling growth

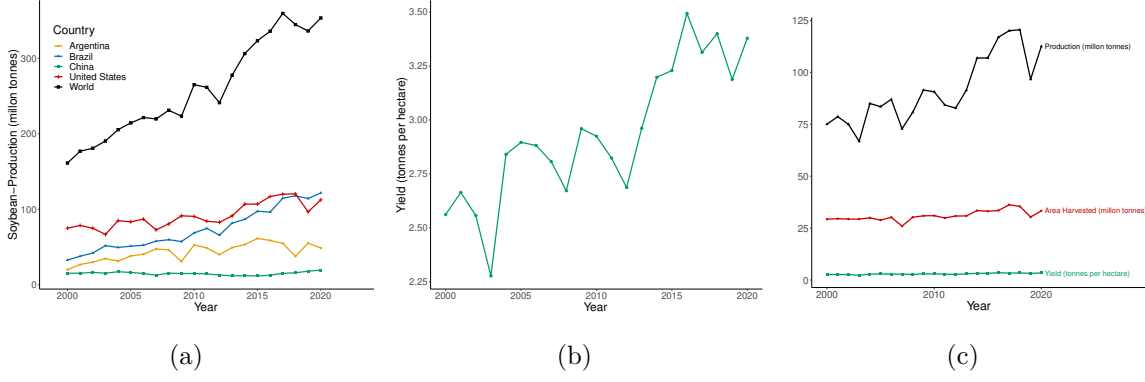


Figure 1: (a) Soybean production data from 2000 to 2020 in the world and the four highest soybean-producing countries, namely the United States, Brazil, Argentina, and China. (b) Soybean yield in the United States from 2000 to 2020. (c) Comparison of soybean production and yield and area harvested in the United States from 2000 to 2020. These data are published by the Food and Agriculture Organization of the United Nations.

in four soybean cultivars, identifying an optimal temperature of approximately 25°C for both processes. Similarly, Alsajri et al. (2022) reported that the optimal temperature range for growth in two selected soybean cultivars was 24°C – 27°C , aligning with the findings of Szczerba et al. (2021). Hence, comprehending the intricate mechanisms of daily temperature, precipitation and irrigation to soybeans is crucial for enhancing both the growth and productivity of soybeans. The traditional approach for examining the correlation between a scalar response variable and combined (functional and scalar) covariates is the functional mean regression. This regression model primarily focuses on the conditional mean of the soybean yield distribution, thereby overlooking the impact of factors on the extremes of the response. However, in agricultural economics, investigations into the upper quantiles of yield hold greater interest and importance. In contrast, functional quantile regression (Chen and Müller, 2012; Kato, 2012) can unveil the influence of covariates on the extreme values of the response variable.

Furthermore, agricultural systems are dynamic, and seasonal variations can lead to sparse regions in the functional coefficient of the functional covariate (e.g. daily temperatures) on the scalar response (soybean yields). By identifying these sparse regions, a deeper

understanding of the variability and dynamics of agricultural systems can be achieved. Effective resource management can also be achieved, e.g., pinpointing these sparse regions can allow farmers to more accurately adjust interventions to reduce input costs such as water and fertilizer, thereby maximizing productivity.

This research is proposed to explore the impact of temperature, precipitation, and irrigation on soybean yield and identify the specific periods during which daily temperature exhibits a non-zero influence on annual soybean yield under different quantile levels. Motivated by this application problem but not limited to solving this one practical problem, we propose the following locally sparse semi-parametric functional quantile model,

$$Q_\tau(Y|\mathbf{Z}, \mathbf{X}(\cdot)) = \mathbf{Z}^T \boldsymbol{\alpha}_\tau + \int_0^T \mathbf{X}^T(t) \boldsymbol{\beta}_\tau(t) dt, \quad (1)$$

where $Q_\tau(Y|\mathbf{Z}, \mathbf{X}(\cdot))$ is the τ -th conditional quantile of the scalar response Y given $\mathbf{X}(\cdot) = (X_1(\cdot), \dots, X_m(\cdot))^T$ and \mathbf{Z} for a fixed quantile level $\tau \in (0, 1)$. Without loss of generality, we assume that the domain for each $X_l(\cdot), l = 1, \dots, m$ is the same, specifically characterized by $t \in [0, \mathcal{T}]$ and $\boldsymbol{\beta}_\tau(\cdot) = (\beta_{\tau,1}(\cdot), \dots, \beta_{\tau,m}(\cdot))^T$ is a vector of corresponding functional coefficients. Meanwhile, some scalar covariates $\mathbf{Z} = (Z_1, \dots, Z_d)^T$ are taken into account in this model and $\boldsymbol{\alpha}_\tau$ is a $d \times 1$ vector of coefficients, where we set $Z_1 \equiv 1$ and $\alpha_{\tau,1}$ denotes the intercept throughout this article. In our soybean application, Y is the annual soybean yield, $X_1(t)$ and $X_2(t)$ are the daily maximum and minimum temperature, respectively, and Z_1 and Z_2 are the annual precipitation and the ratio of irrigated area of each county in Kansas.

The functional coefficient $\beta_{\tau,l}(\cdot)$ is assumed to be locally sparse, which means that $\beta_{\tau,l}(t) = 0$ in some regions \mathcal{N} , where \mathcal{N} is a subset of the whole time domain $[0, \mathcal{T}]$. Then the local sparsity of $\boldsymbol{\beta}_\tau(\cdot)$ can depict the dynamic dependence of the τ -th conditional

quantile of the scalar response Y on the functional covariates.

The proposed sparse semi-parametric functional quantile model (1) includes a variety of functional models as special cases. For example, when the identified sparse regions for all functional coefficient $\beta_{\tau,l}(t), l = 1, \dots, m$, equal to $[0, \mathcal{T}]$, then model (1) becomes the classic quantile regression (Koenker and Bassett Jr, 1978). If $\alpha_{\tau,l} = 0$ for all $l = 1, \dots, d$, and no functional coefficient $\beta_{\tau,l}$ has a locally sparse region, model (1) is reduced to the functional quantile regression (FQR) with only functional covariates (Chen and Müller, 2012; Kato, 2012). Various partially functional quantile regression models are special cases of our proposed model. For instance, Yao et al. (2017) consider a partially functional quantile regression with a functional covariate and high-dimensional scalar covariates. Ma et al. (2019) proposed a functional partially linear model with multiple functional covariates and ultrahigh-dimensional scalar covariates, and imposed two nonconvex penalties to select the significant functional and scalar covariates. To the best of our knowledge, no work has studied the local sparsity structure for functional quantile models, although it is common and important in various applications.

Most existing works considering local sparsity focus on the mean regression models (Wang et al., 2007; James et al., 2009; Zhou et al., 2013). A variety of regularization techniques have been developed to induce the local sparsity of functions. One class of methods leverages the local support property of B-splines combined with group bridge penalties (Huang et al., 2009). For example, Wang and Kai (2015) investigated functional sparsity in nonparametric regression. Building on similar ideas, Tu et al. (2020) studied simultaneous domain selection for nonparametric varying-coefficient models with longitudinal data. In the context of functional linear regression, Guan et al. (2020) focused on

identifying nonzero regions near the boundaries, while Wang et al. (2023) aimed to detect locally sparse supports in function-on-scalar linear regression. Another widely used approach is based on the concave penalty SCAD. Lin et al. (2017) proposed a functional extension of the SCAD penalty (Fan and Li, 2001), known as functional SCAD (fSCAD), to achieve locally sparse estimation in scalar-on-function regression. This method has been further applied in multi-output settings, such as in Li et al. (2022), for functional linear regression with multiple responses. Additionally, Park et al. (2022) developed a regularization method for functional linear discriminant analysis that similarly induces zero-effect regions. While other penalty functions such as the group bridge can also be employed to induce local sparsity, in this paper we primarily adopt the second approach based on the fSCAD penalty.

Our article makes several contributions. First, we propose a locally sparse semi-parametric functional quantile regression model and develop a Convolution-smoothing based Locally Sparse Estimation (CLoSE) method. This unified framework simultaneously selects important functional covariates, identifies locally sparse regions to enhance interpretability, and estimates the corresponding functional coefficients. To alleviate the computational challenges associated with optimizing the piecewise linear quantile loss combined with a concave fSCAD penalty, we adopt a smoothed quantile loss function based on convolution techniques (Fernandes et al., 2021; He et al., 2023; Tan et al., 2022). Second, to provide a rigorous foundation for our approach, we establish several key theoretical results. Specifically, we prove the existence of a local minimizer for the associated optimization problem, ensuring the estimator is well-defined. We further demonstrate that the estimated functional coefficients possess functional oracle properties, including local sparsity and asymp-

otic normality. Consequently, we also derive simultaneous confidence bands (SCBs) for the estimated functional coefficients. Additionally, we establish the asymptotic normality of the model parameters, enabling valid statistical inference. These theoretical guarantees highlight the reliability and practical utility of the proposed method. Finally, the analysis of soybean yield data from Kansas demonstrates that the time periods during which temperature significantly affects yield differ across quantile levels. In particular, different functional climatic factors emerge as significant at different parts of the yield distribution. These insights may inform targeted agricultural strategies, such as temperature regulation during critical growth stages, to optimize crop production.

The remainder of the paper is organized as follows. Section 2 proposes a method for identifying locally sparse regions and estimating functional coefficients on nonnull regions. Section 3 presents the asymptotic properties of the estimators. Section 4 reports the real data analysis, and Section 5 concludes with discussions. Numerical studies, technical conditions, and proofs are provided in the supplementary material.

2 CLoSE Method

2.1 Convolution-type Smoothing Approach

Suppose that $\{(\mathbf{Z}_i, \mathbf{X}_i(t), Y_i, t \in [0, \mathcal{T}])\}_{i=1}^n$ is an independent and identically distributed random sample from $(\mathbf{Z}, \mathbf{X}(t), Y, t \in [0, \mathcal{T}])$. Then the locally sparse FQR estimator can be obtained by minimizing the following loss function

$$\mathcal{L}(\boldsymbol{\alpha}_\tau, \boldsymbol{\beta}_\tau, \gamma_l, \lambda_l) = \frac{1}{n} \sum_{i=1}^n \rho_\tau \left(Y_i - \mathbf{Z}_i^T \boldsymbol{\alpha}_\tau - \int_0^\mathcal{T} \mathbf{X}_i^T(t) \boldsymbol{\beta}_\tau(t) dt \right) + \sum_{l=1}^m \gamma_l \|\mathcal{D}^q \boldsymbol{\beta}_{\tau, l}\|_2^2 + \text{Locally sparse penalty}, \quad (2)$$

where $\rho_\tau(u) = u(\tau - I(u < 0))$ is the quantile check function, and $I(\cdot)$ is an indicator function. However, $\rho_\tau(u)$ is not differentiable at $u = 0$, which poses challenges for optimization and theoretical analysis. In the loss function (2), the second term is a convex roughness penalty with the q th-order differential operator \mathcal{D}^q and the non-negative tuning parameters $\gamma_l, l = 1, \dots, m$, which control the smoothness of the estimated coefficient functions. For the third term, we choose the fSCAD penalty (Lin et al., 2017), which is a concave penalty, to simultaneously identify the zero regions of the estimated functional coefficients and select the significant functional covariates.

The loss function (2) has no closed-form solution. Iterative procedures are often adopted to find the optimal solution. However, in the iterative algorithm for minimizing the loss function (2), the combination of a first-order non-differentiable check function and a concave locally sparse penalty brings computation difficulty. More specifically, local quadratic approximation (LQA) is a commonly used strategy for the optimization that involves fSCAD or SCAD penalty (Fan and Li, 2001; Lin et al., 2017). Such an algorithm usually requires the calculation of gradient and Hessian matrix, which is not available for (2) because of the non-differentiable check function. To make the computation fast and stable, we consider an alternative convolution smoothed quantile loss function (Fernandes et al., 2021; He et al., 2023; Tan et al., 2022).

Let $e(\boldsymbol{\alpha}_\tau, \boldsymbol{\beta}_\tau) = Y - \mathbf{Z}^T \boldsymbol{\alpha}_\tau - \int_0^T \mathbf{X}^T(t) \boldsymbol{\beta}_\tau(t) dt$. Denote the conditional cumulative distribution function (CDF) and density function of $e(\boldsymbol{\alpha}_\tau, \boldsymbol{\beta}_\tau)$ given \mathbf{Z} and $\mathbf{X}(t)$ as $F_{e|\mathbf{Z}, \mathbf{X}}(\cdot)$ and $f_{e|\mathbf{Z}, \mathbf{X}}(\cdot)$, respectively. Then the population quantile loss can be expressed as

$$E[\rho_\tau(\boldsymbol{\alpha}_\tau, \boldsymbol{\beta}_\tau)] = E_{\mathbf{Z}, \mathbf{X}} \left\{ \int \rho_\tau(u) dF_{e|\mathbf{Z}, \mathbf{X}}(u; \boldsymbol{\alpha}_\tau, \boldsymbol{\beta}_\tau) \right\}. \quad (3)$$

When the unknown CDF $F_{e|\mathbf{Z}, \mathbf{X}}(u; \boldsymbol{\alpha}_\tau, \boldsymbol{\beta}_\tau)$ in (3) is replaced by the empirical distribu-

tion function $\widehat{F}(u; \boldsymbol{\alpha}_\tau, \boldsymbol{\beta}_\tau) = 1/n \sum_{i=1}^n I(e_i(\boldsymbol{\alpha}_\tau, \boldsymbol{\beta}_\tau) \leq u)$ of the residuals $e_i(\boldsymbol{\alpha}_\tau, \boldsymbol{\beta}_\tau) = Y_i - \mathbf{Z}_i^T \boldsymbol{\alpha}_\tau - \int_0^T \mathbf{X}_i^T(t) \boldsymbol{\beta}_\tau(t) dt$, we can obtain the standard quantile loss, that is, the first term in (2). However, the empirical distribution function $\widehat{F}(u; \boldsymbol{\alpha}_\tau, \boldsymbol{\beta}_\tau)$ is a discontinuous function. Thus, a kernel smoothing estimator of $F_{e|\mathbf{Z}, \mathbf{X}}(u; \boldsymbol{\alpha}_\tau, \boldsymbol{\beta}_\tau)$ is a better choice (Fernandes et al., 2021; Tan et al., 2022). The kernel density estimator is $\widehat{f}_h(u; \boldsymbol{\alpha}_\tau, \boldsymbol{\beta}_\tau) = 1/n \sum \mathcal{K}_h(u - e_i(\boldsymbol{\alpha}_\tau, \boldsymbol{\beta}_\tau)) = (nh)^{-1} \sum \mathcal{K}((u - e_i(\boldsymbol{\alpha}_\tau, \boldsymbol{\beta}_\tau))/h)$, where $\mathcal{K}(\cdot)$ is a kernel function, h is a bandwidth and $\mathcal{K}_h(u) = 1/h \mathcal{K}(u/h)$. The corresponding kernel smoothing CDF estimator is $\widehat{F}_h(u; \boldsymbol{\alpha}_\tau, \boldsymbol{\beta}_\tau) = n^{-1} \sum G_h(u - e_i(\boldsymbol{\alpha}_\tau, \boldsymbol{\beta}_\tau))$, where $G_h(u) = G(u/h)$ and $G(u) = \int_{-\infty}^u \mathcal{K}(v) dv$. When we replace the unknown CDF by the kernel smoothing estimator of the CDF $\widehat{F}_h(u; \boldsymbol{\alpha}_\tau, \boldsymbol{\beta}_\tau)$, we derive a new loss function with the convolution smoothed quantile loss:

$$\mathcal{L}^*(\boldsymbol{\alpha}_\tau, \boldsymbol{\beta}_\tau, \gamma_l, \lambda_l) = \frac{1}{n} \sum_{i=1}^n (\rho_\tau * \mathcal{K}_h) \left(Y_i - \mathbf{Z}_i^T \boldsymbol{\alpha}_\tau - \int_0^T \mathbf{X}_i^T(t) \boldsymbol{\beta}_\tau(t) dt \right) + \sum_{l=1}^m \gamma_l \|\mathcal{D}^q \beta_{\tau, l}\|_2^2 + \text{fSCAD}, \quad (4)$$

where $(\rho_\tau * \mathcal{K}_h)(u) = \int_{-\infty}^{\infty} \rho_\tau(v) \mathcal{K}_h(v - u) dv$ and $*$ is the convolution operator. The smoothed quantile loss is a global convex function, which has first and second-order derivatives to make the computation faster.

2.2 Estimation Procedure

We use B-spline basis functions to represent the functional coefficients $\beta_{\tau, l}(t), l = 1, \dots, m$. We set the order to be $p + 1$ and place $K + 1$ equally spaced knots $0 = t_0 < t_1 < \dots < t_{K-1} < t_K = \mathcal{T}$ in the domain $[0, \mathcal{T}]$ to define a set of B-spline basis functions. Then the functional coefficient $\beta_{\tau, l}(t)$ can be approximated by the B-spline basis functions $\beta_{\tau, l}(t) \approx \mathbf{B}^T(t) \boldsymbol{\theta}_{\tau, l}$, where $\mathbf{B}(t) = (B_1(t), \dots, B_{K+p}(t))^T$ is the vector of B-spline

basis functions and $\boldsymbol{\theta}_{\tau,l} = (\theta_{\tau,l,1}, \dots, \theta_{\tau,l,K+p})^T$ is the corresponding coefficients. Denote $\mathbf{U}_i = \int_0^\tau \mathbf{X}_i(t) \otimes \mathbf{B}(t) dt$ and $\boldsymbol{\theta}_\tau^T = (\boldsymbol{\theta}_{\tau,1}^T, \dots, \boldsymbol{\theta}_{\tau,m}^T)$, then the first term of $\mathcal{L}^*(\boldsymbol{\alpha}_\tau, \beta_\tau, \gamma, \lambda)$ can be written as $n^{-1} \sum_{i=1}^n (\rho_\tau * \mathcal{K}_h)(Y_i - \mathbf{Z}_i^T \boldsymbol{\alpha}_\tau - \mathbf{U}_i^T \boldsymbol{\theta}_\tau)$. The roughness penalty in (4) can be expressed as

$$\sum_{l=1}^m \gamma_l \left\| \left(\mathbf{B}^{(q)}(t) \right)^T \boldsymbol{\theta}_{\tau,l} \right\|_2^2 = \sum_{l=1}^m \gamma_l \boldsymbol{\theta}_{\tau,l}^T \mathbf{V} \boldsymbol{\theta}_{\tau,l} = \boldsymbol{\theta}_\tau^T (\boldsymbol{\Gamma} \otimes \mathbf{V}) \boldsymbol{\theta}_\tau, \quad (5)$$

where $\boldsymbol{\Gamma} = \text{diag}(\gamma_1, \dots, \gamma_m)$, $\mathbf{V} = \int_0^\tau [\mathbf{B}^{(q)}(t)][\mathbf{B}^{(q)}(t)]^T dt$.

Recall that $0 = t_0 < t_1 < \dots < t_{K-1} < t_K = \mathcal{T}$ is an equally spaced sequence in the domain $[0, \mathcal{T}]$. According to Theorem 1 in Lin et al. (2017), as $K \rightarrow \infty$, the fSCAD penalty term of the l th function $\beta_{\tau,l}(t), t \in [0, \mathcal{T}]$ can be approximated by

$$\frac{K}{\mathcal{T}} \int_0^\tau p_{\lambda_l}(|\beta_{\tau,l}(t)|) dt \approx \sum_{j=1}^K p_{\lambda_l} \left(\sqrt{\frac{K}{\mathcal{T}} \int_{t_{j-1}}^{t_j} \beta_{\tau,l}^2(t) dt} \right), \quad (6)$$

here the SCAD penalty (Fan and Li, 2001) $p_{\lambda_l}(u) = \lambda_l u$ if $0 \leq u \leq \lambda_l$, $p_{\lambda_l}(u) = -(u^2 - 2a\lambda_l u + \lambda_l^2)/(2(a-1))$ if $\lambda_l \leq u \leq a\lambda_l$, and $p_{\lambda_l}(u) = (a+1)\lambda_l^2/2$ if $u \geq a\lambda_l$ with the non-negative tuning parameters a and λ_l . A recommended value for tuning parameter a is 3.7 according to Fan and Li (2001).

The approximation (6) shows that the penalty of $\beta_{\tau,l}(t)$ on the whole domain $[0, \mathcal{T}]$ is equal to the averaged SCAD penalty on each small subinterval $[t_{j-1}, t_j]$. When $\beta_{\tau,l}(t)$ is significant on $[t_{j-1}, t_j]$, then $p_{\lambda_l} \left(\sqrt{\frac{K}{\mathcal{T}} \int_{t_{j-1}}^{t_j} \beta_{\tau,l}^2(t) dt} \right)$ can not over shrink $\beta_{\tau,l}(t), t \in [t_{j-1}, t_j]$. Inversely, when $\beta(t)$ is vary small on the subinterval $[t_{j-1}, t_j]$, the penalty $p_{\lambda_l} \left(\sqrt{\frac{K}{\mathcal{T}} \int_{t_{j-1}}^{t_j} \beta_{\tau,l}^2(t) dt} \right)$ can shrink $\beta_{\tau,l}(t)$ toward zero for every $t \in [t_{j-1}, t_j]$, and then $\beta_{\tau,l}(t)$ is sparse on $[t_{j-1}, t_j]$, which produces a locally sparse estimate. In model (1), there are m -dimensional functional covariates $\mathbf{X}(t)$ and m corresponding functional coefficients $\beta_{\tau,l}, l = 1, \dots, m$. Suppose

different functional coefficients $\beta_{\tau,l}$ have different fSCAD tuning parameters λ_l , thus the fSCAD penalty on all functional coefficients is the summation of the fSCAD penalty on each functional coefficient:

$$\sum_{l=1}^m \frac{K}{\mathcal{T}} \int_0^{\mathcal{T}} p_{\lambda_l}(|\beta_{\tau,l}(t)|) dt \approx \sum_{l=1}^m \sum_{j=1}^K p_{\lambda_l} \left(\sqrt{\frac{K}{\mathcal{T}}} \int_{t_{j-1}}^{t_j} \beta_{\tau,l}^2(t) dt \right). \quad (7)$$

Plugging the spline approximation into $\int_{t_{j-1}}^{t_j} \beta_{\tau,l}^2(t) dt$, we can get the matrix representation, $\int_{t_{j-1}}^{t_j} \beta_{\tau,l}^2(t) dt = \boldsymbol{\theta}_{\tau,l}^T \mathbf{W}_j \boldsymbol{\theta}_{\tau,l}$, where \mathbf{W}_j is an $(K+p)$ by $(K+p)$ matrix with entries $w_{uv} = \int_{t_{j-1}}^{t_j} B_u(t) B_v(t) dt$ if $j \leq u, v \leq j+p$ and zero otherwise. Thus the fSCAD penalty (7) can be rewritten as

$$\sum_{l=1}^m \sum_{j=1}^K p_{\lambda_l} \left(\sqrt{\frac{K}{\mathcal{T}}} \int_{t_{j-1}}^{t_j} \beta_{\tau,l}^2(t) dt \right) = \sum_{l=1}^m \sum_{j=1}^K p_{\lambda_l} \left(\sqrt{\frac{K}{\mathcal{T}}} \boldsymbol{\theta}_{\tau,l}^T \mathbf{W}_j \boldsymbol{\theta}_{\tau,l} \right). \quad (8)$$

Then, combined with the B-spline approximation, (5) and (8), we can rewrite the loss function (4) as follows,

$$\mathcal{L}^*(\boldsymbol{\alpha}_{\tau}, \boldsymbol{\theta}_{\tau}, \gamma_l, \lambda_l) \approx \frac{1}{n} \sum_{i=1}^n (\rho_{\tau} * \mathcal{K}_h)(Y_i - \mathbf{Z}_i^T \boldsymbol{\alpha}_{\tau} - \mathbf{U}_i^T \boldsymbol{\theta}_{\tau}) + \boldsymbol{\theta}_{\tau}^T (\boldsymbol{\Gamma} \otimes \mathbf{V}) \boldsymbol{\theta}_{\tau} + \sum_{l=1}^m \sum_{j=1}^K p_{\lambda_l} \left(\sqrt{\frac{K}{\mathcal{T}}} \boldsymbol{\theta}_{\tau,l}^T \mathbf{W}_j \boldsymbol{\theta}_{\tau,l} \right). \quad (9)$$

Overall, both the roughness penalty and the locally sparse penalty (fSCAD) serve as regularization mechanisms, each with a corresponding tuning parameter that governs its strength. These penalties play complementary roles in balancing model flexibility, smoothness, and interpretability. The roughness penalty controls the global smoothness of the estimated functional coefficients $\beta_{\tau,l}(t)$ with tuning parameters γ_l . A larger γ_l enforces greater smoothness, reducing variance but potentially introducing bias by oversmoothing important features. A smaller γ_l allows more flexibility but may lead to overfitting, especially in noisy data. The fSCAD penalty with the tuning parameters λ_l , on the other hand,

promotes sparsity in the functional domain by shrinking the functional coefficients toward zero in specific subintervals the tuning parameter associated with sparsity. A larger λ_l encourages more aggressive local shrinkage, potentially setting large portions of the functions to zero and improving interpretability. A smaller λ_l allows for more detailed estimation but may retain irrelevant regions of the function, increasing model complexity. When used jointly, γ_l , $l = 1, \dots, m$ and λ_l , $l = 1, \dots, m$ provide a flexible framework for estimating functional coefficients that are both smooth and locally sparse.

However, the SCAD penalty $p_{\lambda_l}(\cdot)$ is not differentiable, which brings difficulty in the optimization. There are two ways to approximate $p_{\lambda_l}(\cdot)$, local quadratic approximation (LQA; Fan and Li 2001) and local linear approximation (LLA; Zou and Li (2008)). Lin et al. (2017) found that LLA does not work well with L^q norm of functions and they suggested using LQA in their paper. Therefore, we also choose the LQA to approximate the fSCAD penalty. When $u \approx u^{(0)}$, the LQA of the SCAD function $p_{\lambda_l}(u)$ is:

$$\begin{aligned} p_{\lambda_l}(|u|) &\approx p_{\lambda_l}(|u^{(0)}|) + \frac{1}{2} \frac{\dot{p}_{\lambda_l}(|u^{(0)}|)}{|u^{(0)}|} (u^2 - u^{(0)2}) = \frac{1}{2} \frac{\dot{p}_{\lambda_l}(|u^{(0)}|)}{|u^{(0)}|} u^2 + p_{\lambda_l}(|u^{(0)}|) - \frac{1}{2} \frac{\dot{p}_{\lambda_l}(|u^{(0)}|)}{|u^{(0)}|} u^{(0)2} \\ &\triangleq \frac{1}{2} \frac{\dot{p}_{\lambda_l}(u^{(0)})}{|u^{(0)}|} u^2 + R_1(u^{(0)}), \end{aligned} \quad (10)$$

where $\dot{p}_{\lambda_l}(u)$ is the first order derivative of $p_{\lambda_l}(u)$ and $R_1(u^{(0)})$ is a constant of $u^{(0)}$.

Then given some initial estimator $\hat{\boldsymbol{\theta}}_\tau^{(0)} = (\hat{\boldsymbol{\theta}}_{\tau,1}^{(0)T}, \dots, \hat{\boldsymbol{\theta}}_{\tau,m}^{(0)T})^T$, when $\boldsymbol{\theta}_\tau \approx \hat{\boldsymbol{\theta}}_\tau^{(0)}$, we have

$$\begin{aligned} \sum_{l=1}^m \sum_{j=1}^K p_{\lambda_l} \left(\sqrt{\frac{K}{\mathcal{T}}} \boldsymbol{\theta}_{\tau,l}^T \mathbf{W}_j \boldsymbol{\theta}_{\tau,l} \right) &\approx \frac{1}{2} \sum_{l=1}^m \sum_{j=1}^K \frac{\dot{p}_{\lambda_l} \left(\sqrt{\frac{K}{\mathcal{T}}} \hat{\boldsymbol{\theta}}_{\tau,l}^{(0)T} \mathbf{W}_j \hat{\boldsymbol{\theta}}_{\tau,l}^{(0)} \right)}{\sqrt{\frac{K}{\mathcal{T}}} \hat{\boldsymbol{\theta}}_{\tau,l}^{(0)T} \mathbf{W}_j \hat{\boldsymbol{\theta}}_{\tau,l}^{(0)}} \frac{\boldsymbol{\theta}_{\tau,l}^T \mathbf{W}_j \boldsymbol{\theta}_{\tau,l}}{\mathcal{T}/K} + R_2(\hat{\boldsymbol{\theta}}_\tau^{(0)}) \\ &\approx \frac{1}{2} \sum_{l=1}^m \sum_{j=1}^K \frac{\dot{p}_{\lambda_l} \left(\sqrt{\frac{K}{\mathcal{T}}} \hat{\boldsymbol{\theta}}_{\tau,l}^{(0)T} \mathbf{W}_j \hat{\boldsymbol{\theta}}_{\tau,l}^{(0)} \right)}{\sqrt{\frac{\mathcal{T}}{K}} \hat{\boldsymbol{\theta}}_{\tau,l}^{(0)T} \mathbf{W}_j \hat{\boldsymbol{\theta}}_{\tau,l}^{(0)}} \boldsymbol{\theta}_{\tau,l}^T \mathbf{W}_j \boldsymbol{\theta}_{\tau,l} + R_2(\hat{\boldsymbol{\theta}}_\tau^{(0)}), \end{aligned} \quad (11)$$

where

$$R_2(\hat{\boldsymbol{\theta}}_\tau^{(0)}) = \sum_{l=1}^m \sum_{j=1}^K p_{\lambda_l} \left(\sqrt{\frac{K}{\mathcal{T}}} \hat{\boldsymbol{\theta}}_{\tau,l}^{(0)T} \mathbf{W}_j \hat{\boldsymbol{\theta}}_{\tau,l}^{(0)} \right) - \frac{1}{2} \sum_{l=1}^m \sum_{j=1}^K \dot{p}_{\lambda_l} \left(\sqrt{\frac{K}{\mathcal{T}}} \hat{\boldsymbol{\theta}}_{\tau,l}^{(0)T} \mathbf{W}_j \hat{\boldsymbol{\theta}}_{\tau,l}^{(0)} \right) \sqrt{\frac{K}{\mathcal{T}}} \hat{\boldsymbol{\theta}}_{\tau,l}^{(0)T} \mathbf{W}_j \hat{\boldsymbol{\theta}}_{\tau,l}^{(0)},$$

only depends on the initial estimator $\widehat{\boldsymbol{\theta}}_\tau^{(0)}$. Denote

$$\mathbf{W}_{\tau,l}^{(0)} = \frac{1}{2} \sum_{j=1}^K \frac{\dot{p}_{\lambda_l} \left(\sqrt{\frac{K}{\mathcal{T}} \widehat{\boldsymbol{\theta}}_{\tau,l}^{(0)T} \mathbf{W}_j \widehat{\boldsymbol{\theta}}_{\tau,l}^{(0)}} \right)}{\sqrt{\frac{\mathcal{T}}{K} \widehat{\boldsymbol{\theta}}_{\tau,l}^{(0)T} \mathbf{W}_j \widehat{\boldsymbol{\theta}}_{\tau,l}^{(0)}}} \mathbf{W}_j, \quad \text{and} \quad \mathbf{W}_\tau^{(0)} = \begin{pmatrix} \mathbf{w}_{\tau,1}^{(0)} & & \\ & \ddots & \\ & & \mathbf{w}_{\tau,m}^{(0)} \end{pmatrix},$$

we can get $\sum_{l=1}^m \sum_{j=1}^K p_{\lambda_l} \left(\sqrt{K/\mathcal{T} \boldsymbol{\theta}_\tau^T \mathbf{W}_j \boldsymbol{\theta}_\tau} \right) \approx \boldsymbol{\theta}_\tau^T \mathbf{W}_\tau^{(0)} \boldsymbol{\theta}_\tau + R_2(\widehat{\boldsymbol{\theta}}_\tau^{(0)})$. Thus we can express the loss function (9) as follows,

$$\mathcal{L}^*(\boldsymbol{\alpha}_\tau, \boldsymbol{\theta}_\tau, \gamma_l, \lambda_l \mid \widehat{\boldsymbol{\theta}}_\tau^{(0)}) \approx \frac{1}{n} \sum_{i=1}^n (\rho_\tau * \mathcal{K}_h)(Y_i - \mathbf{Z}_i^T \boldsymbol{\alpha}_\tau - \mathbf{U}_i^T \boldsymbol{\theta}_\tau) + \boldsymbol{\theta}_\tau^T (\boldsymbol{\Gamma} \otimes \mathbf{V}) \boldsymbol{\theta}_\tau + \boldsymbol{\theta}_\tau^T \mathbf{W}_\tau^{(0)} \boldsymbol{\theta}_\tau + R_2(\widehat{\boldsymbol{\theta}}_\tau^{(0)}). \quad (12)$$

Denote $\mathcal{L}_0^*(\boldsymbol{\alpha}_\tau, \boldsymbol{\theta}_\tau) = 1/n \sum_{i=1}^n (\rho_\tau * \mathcal{K}_h)(Y_i - \mathbf{Z}_i^T \boldsymbol{\alpha}_\tau - \mathbf{U}_i^T \boldsymbol{\theta}_\tau)$, we can get the first-order and second-order derivatives of $\mathcal{L}_0^*(\boldsymbol{\alpha}_\tau, \boldsymbol{\theta}_\tau)$ respectively, that is, $\dot{\mathcal{L}}_0^*(\boldsymbol{\alpha}_\tau, \boldsymbol{\theta}_\tau) = 1/n \sum_{i=1}^n \{G_h(\mathbf{Z}_i^T \boldsymbol{\alpha}_\tau + \mathbf{U}_i^T \boldsymbol{\theta}_\tau - Y_i) - \tau\} (\mathbf{Z}_i^T, \mathbf{U}_i^T)^T$, $\ddot{\mathcal{L}}_0^*(\boldsymbol{\alpha}_\tau, \boldsymbol{\theta}_\tau) = 1/n \sum_{i=1}^n \mathcal{K}_h(\mathbf{Z}_i^T \boldsymbol{\alpha}_\tau + \mathbf{U}_i^T \boldsymbol{\theta}_\tau - Y_i) (\mathbf{Z}_i^T, \mathbf{U}_i^T)^T (\mathbf{Z}_i^T, \mathbf{U}_i^T)^T$.

With the smoothed quantile loss and LQA on the fSCAD penalty, we are able to calculate its gradient and Hessian matrix. Then an iterative NewtonRaphson type algorithm can be used to solve the optimization problem. More specifically, for a fixed $\mathbf{W}_\tau^{(k)}$, we use a NewtonRaphson type algorithm to solve the minimization of $\mathcal{L}^*(\boldsymbol{\alpha}_\tau, \boldsymbol{\theta}_\tau, \gamma_l, \lambda_l \mid \widehat{\boldsymbol{\theta}}_\tau^{(k)})$ with respect to $(\boldsymbol{\alpha}_\tau, \boldsymbol{\theta}_\tau)$. After it converges, we update $\mathbf{W}_\tau^{(k)}$ to $\mathbf{W}_\tau^{(k+1)}$ and then minimize $\mathcal{L}^*(\boldsymbol{\alpha}_\tau, \boldsymbol{\theta}_\tau, \gamma_l, \lambda_l \mid \widehat{\boldsymbol{\theta}}_\tau^{(k+1)})$. We repeat this procedure until the sequences of minimizers $(\boldsymbol{\alpha}_\tau^{(j)}, \boldsymbol{\theta}_\tau^{(j)})$ converge. Note that in practice, the term $\dot{p}_{\lambda_l}(u^{(0)})/|u^{(0)}|$ in (10) can go to infinity if $|u^{(0)}|$ is very small, which can cause the algorithm to be unstable. To solve this issue, we adopt the modified LQA procedure from Hunter and Li (2005) for $p_{\lambda_l}(\cdot)$. We summarize the computational details in Section S1 of the supplementary document.

Let S_1 and S_2 denote the candidate sets for the tuning parameters λ_l and γ_l , respectively. We tune these parameters based on the following strategy. For a given pair (λ_l, γ_l) , with $\lambda_l \in S_1$ and $\gamma_l \in S_2$, we first fit model (12) to identify the estimated null and non-null subregions,

denoted by $\widehat{\mathcal{N}}(\beta_{\tau,l})$ and $\widehat{\mathcal{S}}(\beta_{\tau,l})$, respectively. Next, we refit model (12) using only the data within the estimated signal region $\widehat{\mathcal{S}}(\beta_{\tau,l})$, i.e., $\mathbf{X}_i(t)$ for $t \in \widehat{\mathcal{S}}(\beta_{\tau,l})$, and without applying the fSCAD penalty. We then evaluate each candidate pair (λ_l, γ_l) using the Bayesian Information Criterion (BIC) (Lee et al., 2014), and select the pair that minimizes the BIC.

3 Large Sample Properties

For any vector, we shall use $\|\cdot\|_2$ to denote the Euclidean norm. The null region and nonnull region of $\beta_{\tau,l}(t), l = 1, \dots, m$ are denoted by $\mathcal{N}(\beta_{\tau,l})$ and $\mathcal{S}(\beta_{\tau,l})$, respectively, where $\mathcal{N}(\beta_{\tau,l}) = \{t \in [0, \mathcal{T}] : \beta_{\tau,l}(t) = 0\}$ and $\mathcal{S}(\beta_{\tau,l}) = \{t \in [0, \mathcal{T}] : \beta_{\tau,l}(t) \neq 0\}$. $\mathbf{B}_{\tau,l,1}(t)$ denotes the $K_{\tau,l}^*$ dimensional sub-vector of $\mathbf{B}(t)$ such that each $B_j(t)$ in $\mathbf{B}_{\tau,l,1}(t)$ has a support inside $\mathcal{S}(\beta_{\tau,l})$. Let \mathbf{U}_{τ}^* and $\mathbf{U}_{\tau,i}^*$ be a $K_{\tau}^* = \sum_{l=1}^m K_{\tau,l}^*$ dimensional vector of the corresponding elements of \mathbf{U} and \mathbf{U}_i , respectively, associated with $\mathbf{B}_{\tau,1,1}, \dots, \mathbf{B}_{\tau,m,1}$, where $\mathbf{U} = \int_0^{\mathcal{T}} \mathbf{X}(t) \otimes \mathbf{B}(t) dt$. We also define $\mathbf{Z}_{\tau}^* = (\mathbf{Z}^T, \mathbf{U}_{\tau}^{*T})^T$, $\Sigma_{\tau,1} = E\{\mathbf{Z}_{\tau}^* \mathbf{Z}_{\tau}^{*T}\}$ and $\Sigma_{\tau,2} = E\{f_{e|\mathbf{Z},\mathbf{X}}(0) \mathbf{Z}_{\tau}^* \mathbf{Z}_{\tau}^{*T}\}$. All the technical conditions needed for the theorems are listed in Section S2 of the supplementary document.

3.1 Functional Oracle Property and Asymptotic Normality

It is important to note that all theoretical results in this section rely on the assumption that the tuning parameters for the roughness penalty and the fSCAD penalty satisfy Conditions 5 and 9, respectively, and are assumed to be fixed and known.

Theorem 1. Under Conditions 1-9, there exists a local minimizer $(\widehat{\boldsymbol{\alpha}}_{\tau}, \widehat{\boldsymbol{\beta}}_{\tau})$ of (4) such that $\|\widehat{\boldsymbol{\alpha}}_{\tau} - \boldsymbol{\alpha}_{\tau}\|_2 = O_p(n^{-1/2})$ and $\|\widehat{\boldsymbol{\beta}}_{\tau} - \boldsymbol{\beta}_{\tau}\|_2 = O_p(n^{-1/2} K^{1/2})$.

From this theorem, it is clear that there exists a root- n consistent estimator $\widehat{\boldsymbol{\alpha}}_{\tau}$ and a root- n/K consistent estimator $\widehat{\boldsymbol{\beta}}_{\tau}(t)$.

Theorem 2 (Functional Oracle Property). If Conditions 1-9 hold, as $n \rightarrow \infty$:

- (i) **Locally Sparsity:** For every t not in the support of $\beta_{\tau,l}(t)$, we have $\widehat{\beta}_{\tau,l}(t) = 0$ with probability tending to one.
- (ii) **Asymptotic Normality:** For t such that $\beta_{\tau,l}(t) \neq 0$ we have $\sigma_{\tau,l}^{-1/2}(t)(\widehat{\beta}_{\tau,l}(t) - \beta_{\tau,l}(t)) \xrightarrow{d} \mathbb{G}(t)$, where $\sigma_{\tau,l}(t) = \tau(1 - \tau)\mathbf{\Lambda}_{\tau,l}(t)\mathbf{\Sigma}_{\tau,2}^{-1}(\mathbf{\Sigma}_{\tau,1}/n)\mathbf{\Sigma}_{\tau,2}^{-1}\mathbf{\Lambda}_{\tau,l}^T(t)$, $\mathbf{\Lambda}_{\tau,l}(t) = \boldsymbol{\xi}_l^T \widetilde{\mathbf{B}}_{\tau}(t)(\mathbf{0}_{K_{\tau}^* \times d}, \mathbf{I}_{K_{\tau}^*})$, $\boldsymbol{\xi}_l$ is a $m \times 1$ unit vector in which the l -th element is 1, \mathbf{I}_d be a $d \times d$ identity matrix, $\mathbf{0}_{d \times K_{\tau}^*}$ is a $d \times K_{\tau}^*$ zero matrix, $\widetilde{\mathbf{B}}_{\tau,1}(t) = \text{Bdiag}(\mathbf{B}_{\tau,1,1}^T(t), \dots, \mathbf{B}_{\tau,m,1}^T(t))$, and $\mathbb{G}(t)$ is a Gaussian random process with mean 0 defined on $S(\beta_{\tau,l})$ with the covariance function $\mathcal{C}(t, s) = \tau(1 - \tau)\sigma_{\tau,l}^{-1/2}(t)\sigma_{\tau,l}^{-1/2}(s)\mathbf{\Lambda}_{\tau,l}(t)\mathbf{\Sigma}_{\tau,2}^{-1}(\mathbf{\Sigma}_{\tau,1}/n)\mathbf{\Sigma}_{\tau,2}^{-1}\mathbf{\Lambda}_{\tau,l}^T(s)$.

Theorem 3 (Asymptotic Normality of the Estimators of Parameters). If Conditions 1-9 hold, as $n \rightarrow \infty$, we have $\sqrt{n}(\widehat{\boldsymbol{\alpha}}_{\tau} - \boldsymbol{\alpha}_{\tau}^0) \xrightarrow{d} \mathbb{N}(\mathbf{0}, \tau(1 - \tau)\mathbf{I}_{\tau}\mathbf{\Sigma}_{\tau,2}^{-1}\mathbf{\Sigma}_{\tau,1}\mathbf{\Sigma}_{\tau,2}^{-1}\mathbf{I}_{\tau}^T)$, where $\boldsymbol{\alpha}_{\tau}^0$ is the true parameters and $\mathbf{I}_{\tau} = (\mathbf{I}_d, \mathbf{0}_{d \times K_{\tau}^*})$.

Remark 1. Theorem 2 shows that the estimators $\widehat{\beta}_{\tau}(t)$ possess the functional version oracle property, which makes the fitted model simpler and more interpretable. Denote the left endpoint and right endpoint of $\mathcal{S}(\beta_{\tau,l})$ as $\mathcal{S}^L(\beta_{\tau,l})$ and $\mathcal{S}^R(\beta_{\tau,l})$, respectively. Then we partition $\mathcal{S}(\beta_{\tau,l})$ into $\widetilde{K}_{\tau,l} + 1$ equally spaced intervals with $\mathcal{S}^L(\beta_{\tau,l}) = \nu_0 < \nu_1 < \dots < \nu_{\widetilde{K}_{\tau,l}} < \nu_{\widetilde{K}_{\tau,l}+1} = \mathcal{S}^R(\beta_{\tau,l})$, where $\widetilde{K}_{\tau,l} \rightarrow \infty$. From Theorem 2, we have that for any $a \in (0, 1)$, $\lim_{n \rightarrow \infty} P \left\{ \sup_{t \in \mathcal{S}_{\varepsilon}(\beta_{\tau,l})} \left| \sigma_{\tau,l}^{-1/2}(t) \left\{ \widehat{\beta}_{\tau,l}(t) - \beta_{\tau,l}(t) \right\} \right| \leq \mathcal{Q}_{\tau,l}(a) \right\} = 1 - a$, where $\mathcal{S}_{\varepsilon}(\beta_{\tau,l}) = \{\nu_0, \dots, \nu_{\widetilde{K}_{\tau,l}+1}\}$ as a subset of $\mathcal{S}(\beta_{\tau,l})$ becomes denser as $n \rightarrow \infty$, $\mathcal{Q}_{\tau,l}(a) = (2 \log |\mathcal{S}_{\varepsilon}(\beta_{\tau,l})|)^{1/2} - (2 \log |\mathcal{S}_{\varepsilon}(\beta_{\tau,l})|)^{-1/2} \{ \log(-0.5 \log(1 - a)) + 0.5 [\log(\log |\mathcal{S}_{\varepsilon}(\beta_{\tau,l})|) + \log(4\pi)] \}$, and $|\mathcal{S}_{\varepsilon}(\beta_{\tau,l})|$ denote the cardinality of the set $|\mathcal{S}_{\varepsilon}(\beta_{\tau,l})|$. Then an asymptotic $100(1 - a)\%$ simultaneous confidence band (SCB) for $\beta_{\tau,l}(t)$ over $\mathcal{S}_{\varepsilon}(\beta_{\tau,l})$ is given by $\widehat{\beta}_{\tau,l}(t) \pm \sigma_{\tau,l}^{1/2}(t) \mathcal{Q}_{\tau,l}(a)$.

In addition, for any given fixed point t such that $\beta_{\tau,l}(t) \neq 0$, we have $\sigma_{\tau,l}^{-1/2}(t)(\widehat{\beta}_{\tau,l}(t) - \beta_{\tau,l}(t)) \xrightarrow{d} \mathbb{N}(\mathbf{0}, 1)$, then the asymptotic 100(1 - a)% point-wise confidence band (PCB) of $\beta_{\tau,l}$ is $\widehat{\beta}_{\tau,l}(t) \pm \sigma_{\tau,l}^{1/2}(t)z_{a/2}$ and the width of SCB is inflated by $\mathcal{Q}_{\tau,l}(a)/z_{a/2}$, where $z_{a/2}$ is the upper $a/2$ -quantile of the standard normal distribution.

Theorem 3 establishes the asymptotic normality of the parameters $\alpha_{\tau,l}$ and its corresponding 100(1 - a)% point-wise confidence interval is $\widehat{\alpha}_{\tau,l} \pm n^{-1/2} \sqrt{\tau(1-\tau)\widetilde{\boldsymbol{\xi}}_l^T \boldsymbol{\mathcal{I}}_{\tau} \boldsymbol{\Sigma}_{\tau,2}^{-1} \boldsymbol{\Sigma}_{\tau,1} \boldsymbol{\Sigma}_{\tau,2}^{-1} \boldsymbol{\mathcal{I}}_{\tau}^T \widetilde{\boldsymbol{\xi}}_l} z_{a/2}$, where $\widetilde{\boldsymbol{\xi}}_l$ is a $d \times 1$ unit vector in which the l -th element is 1 and $l = 1, \dots, d$.

3.2 Wild Bootstrap

In Theorems 2 and 3, the covariance function of $\widehat{\beta}_{\tau,l}(t)$: $\mathcal{C}(t, s) = \tau(1-\tau)\sigma_{\tau,l}^{-1/2}(t)\sigma_{\tau,l}^{-1/2}(s)\boldsymbol{\Lambda}_{\tau,l}(t)\boldsymbol{\Sigma}_{\tau,2}^{-1}(\boldsymbol{\Sigma}_{\tau,1}/n)\boldsymbol{\Sigma}_{\tau,2}^{-1}\boldsymbol{\Lambda}_{\tau,l}^T(s)$ and the covariance matrix of $\widehat{\boldsymbol{\alpha}}_{\tau}$: $n^{-1}\tau(1-\tau)\boldsymbol{\mathcal{I}}_{\tau}\boldsymbol{\Sigma}_{\tau,2}^{-1}\boldsymbol{\Sigma}_{\tau,1}\boldsymbol{\Sigma}_{\tau,2}^{-1}\boldsymbol{\mathcal{I}}_{\tau}^T$ are both unknown because that $\boldsymbol{\Sigma}_{\tau,1} = E\{\mathbf{Z}_{\tau}^*\mathbf{Z}_{\tau}^{*T}\}$ and $\boldsymbol{\Sigma}_{\tau,2} = E\{f_{e|\mathbf{Z},\mathbf{X}}(0)\mathbf{Z}_{\tau}^*\mathbf{Z}_{\tau}^{*T}\}$ are both unknown. Estimating the unknown conditional density function of the error given both scalar and functional covariates is particularly challenging, making accurate estimation of the covariance function and matrix essential before constructing SCBs and pointwise confidence intervals. Motivated by the wild bootstrap for classical quantile regression (Feng et al., 2011) and the refitted wild bootstrap for high-dimensional quantile regression (Cheng et al., 2022), we propose a modified wild bootstrap procedure for sparse semiparametric functional quantile regression to simultaneously estimate the covariance function of $\widehat{\beta}_{\tau,l}(t)$ and the covariance matrix of $\widehat{\boldsymbol{\alpha}}_{\tau}$. Detailed steps are provided in Section S3 of the supplementary document.

Theorem 4. Under the Conditions 1-9, using the wild bootstrap procedure, we have

$$\sup_{u \in \mathbb{R}} \left| P \left\{ \sup_{t \in \mathcal{S}_{\varepsilon}(\beta_{\tau,l})} \sqrt{n/K} (\widehat{\beta}_{\tau,l}^{(b)}(t) - \widehat{\beta}_{\tau,l}(t)) \leq u \right\} - P \left\{ \sup_{t \in \mathcal{S}_{\varepsilon}(\beta_{\tau,l})} \sqrt{n/K} (\widehat{\beta}_{\tau,l}(t) - \beta_{\tau,l}(t)) \leq u \right\} \right| \rightarrow 0, \text{ and } \sup_{v \in \mathbb{R}} \left| P(n^{1/2}(\widehat{\alpha}_{\tau,l}^{(b)} - \widehat{\alpha}_{\tau,l}) \leq v) - P(n^{1/2}(\widehat{\alpha}_{\tau,l} - \alpha_{\tau,l}^0) \leq v) \right| \rightarrow 0.$$

Theorem 4 provides a theoretical justification for using the wild bootstrap method to estimate the sample covariance function and covariance matrix for conducting statistical inference.

4 Soybean Yield Data Analysis

In this section, we apply the proposed locally sparse functional quantile regression model to study the relationship between soybean yield and daily temperature profiles, including both maximum and minimum temperatures. Functional quantile regression is particularly suitable in this context as it allows us to investigate how different parts of the temperature curve influence the conditional quantiles of crop yield, capturing both central tendencies and extreme responses. The locally sparse penalty plays a key role by enabling automatic identification of critical time intervals during the growing season when temperature has a significant effect on yield. Moreover, we further utilize the simultaneous confidence bands derived in the theoretical section to perform inference analysis in this real-world application, demonstrating the practical utility of our theoretical developments.

Climate factors such as temperature and rainfall have significant effects on soybean germination and growth. In North America, these climate factors can account for 15% variation of the soybean yield (Vogel et al., 2019). For the stability of soybean production, it is important to keep tracking these factors over the growing season. If we can figure out when and how the temperatures combined with other environmental and non-environmental factors influence the soybean yield, then we may obtain a better soybean planting and harvesting strategy. We can also make some interventions when the temperature is too low or too high. In addition, to have a more thorough understanding of this

relationship, analyzing the conditional quantiles of soybean yield should be more meaningful than analyzing the conditional mean only. For these reasons, in this analysis, we want to identify the impact of daily minimum and daily maximum temperatures on the soybean yield for different quantiles.

Kansas in the United States has 4.7 million acres of soybean planted, producing 200 million bushels, and ranks 10th in the United States in terms of soybean yield. The data on soybean yield and other related non-environmental variables in Kansas state between 1991 and 2006 are collected and organized from the United States Department of Agriculture (USDA) website (<https://quickstats.nass.usda.gov/>). The corresponding measurements on climate variables are collected from the National Oceanic and Atmospheric Administration (NOAA) website (<https://www.ncei.noaa.gov/products>) for Kansas within the same time range.

To be more specific, the soybean yield-related data collected from the USDA website contains the county-level annual soybean yield (measured in bushels per acre), the size of harvested land and the size of irrigated area among each harvested land. The climate data collected from the NOAA website contains daily minimum temperatures, daily maximum temperatures and annual precipitations at the climate station level. To link the observations from different websites together, we first identify the latitudes and longitudes of each climate station and the center of each county of Kansas. Next, we label the location of each climate station by comparing its distance to all the county centers. More specifically, for each climate station, the closest county center is its label of location. To obtain the county-level daily minimum and maximum temperature and annual precipitation observations, we average the corresponding climate station level observations over all the climate stations

within each county. In this way, we integrate all the observations at the county level. Also note that the data set from the USDA website only includes observation of a number of counties for each year in Kansas but not all of them. In the following analysis, we treat the annual precipitation, and the ratio of the size of the irrigated area over the size of harvested land of each county as two scalar predictors and we treat daily minimum temperature and daily maximum temperature curves as two functional predictors. Figure 2 displays a sample of the daily minimum temperature and daily maximum temperature curves of Kansas.

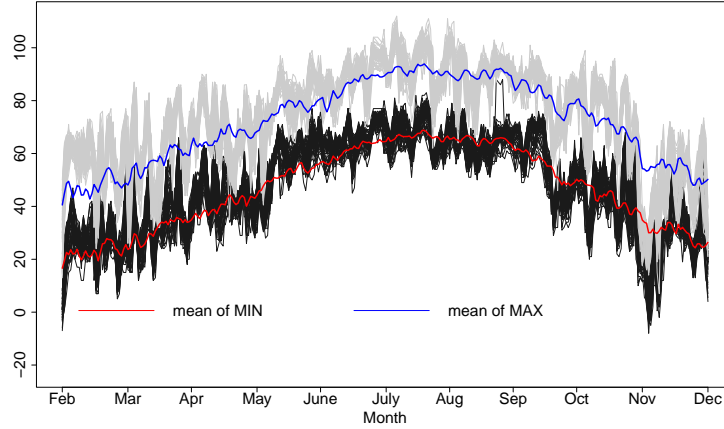


Figure 2: A sample of daily minimum and maximum temperature curves of counties in Kansas. The unit of the y-axis is the Fahrenheit temperature scale.

Let $X_1(t)$ and $X_2(t)$ denote the daily maximum temperature and daily minimum temperature between February and November respectively. Let Z_1 and Z_2 denote the annual precipitation and the ratio of irrigated area of each county in Kansas. Let Y denote the annual soybean yield of each county in Kansas. The model we want to investigate is $Q_\tau(Y|X_1(\cdot), X_2(\cdot), Z_1, Z_2) = c(\tau) + \alpha_{1,\tau}Z_1 + \alpha_{2,\tau}Z_2 + \int_{\mathcal{T}} X_1(t)\beta_{1,\tau}(t)dt + \int_{\mathcal{T}} X_2(t)\beta_{2,\tau}(t)dt$. We fit the model at three different quantiles $\tau = 0.25, 0.5, 0.75$, which represent three different scenarios of the soybean yield: the “worst” case, the normal case and the “best” case. We apply the bootstrap procedure mentioned above to compute the simultaneous confident

bands for $\beta_{1,\tau}$ and $\beta_{2,\tau}$, and the 90%-confidence intervals for $\alpha_{1,\tau}$ and $\alpha_{2,\tau}$.

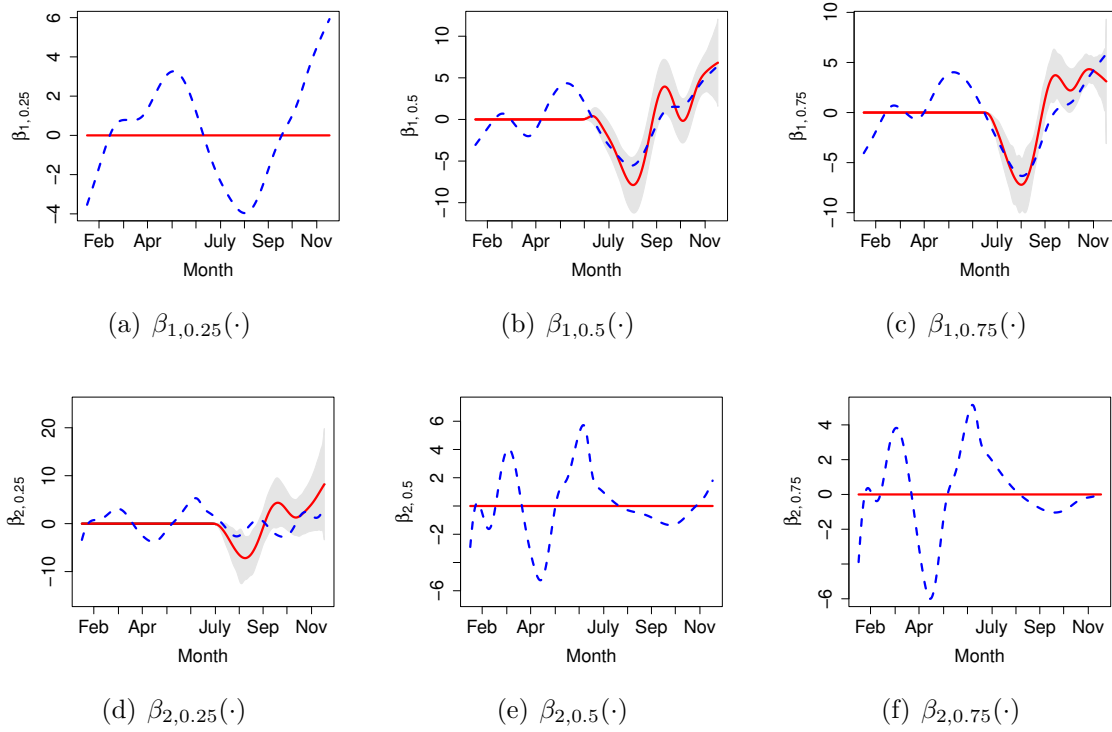


Figure 3: The estimated slope functions using the convolution-smoothing based locally sparse estimation (CLoSE) method (red solid line) and the smoothed quantile loss (SQL) method (blue dashed line) at different quantile levels, $\tau = 0.25, 0.50$ and 0.75 , from the soybean dataset of Kansas. The gray areas are the corresponding 95% simultaneous confidence bands.

Figure 3 displays the simultaneous confident bands for $\beta_{1,\tau}$ and $\beta_{2,\tau}$ with $\tau = 0.25, 0.5$ and 0.75 . Specifically, Figure 3-(a) and Figure 3-(d) show that the daily maximum temperature has no influence on the 25% quantile of the soybean yield. Only the daily minimum temperature after late July matters for this “worst” scenario of the soybean yield. From Figure 3-(e) and Figure 3-(f), we observe that the daily minimum temperature has no effect on the soybean yield for the 50% and 75% quantiles of the soybean yield. On the other hand, Figure 3-(b) and Figure 3-(c) show that the daily maximum temperatures play an important role in these two quantiles of the soybean yield. More specifically, from Figure 3-(b) and Figure 3-(c), we can observe that regarding the 50% and 75% quantiles of the soybean yield, the maximum temperature during the hot summer has a negative effect

and the maximum temperature during the fall and winter have a positive influence. This may be due to the fact that before reaching $30^{\circ}C$ ($86^{\circ}F$), the increasing air temperature can lead to an increase in soybean yield. But after reaching $30^{\circ}C$ ($86^{\circ}F$), a higher temperature is negatively related to the soybean yield (Schlenker and Roberts, 2009). According to the information from the website https://webapp.agron.ksu.edu/agr_social/m_eu_article.throck?article_id=1152, the most active soybean planting dates of different counties of Kansas range from mid-May to late June. This can explain why we observe the sparsity of $\hat{\beta}_{1,\tau}(t)$ and $\hat{\beta}_{2,\tau}(t)$ between February and late June. In addition, the proposed CLoSE method tends to use only one of the two functional predictors: daily minimum and daily maximum temperature curves. This may be due to the high correlation of these two functional predictors. The two predictors may contain repetitive information and therefore using only one of them in the model should be enough. While the SQL method uses whichever predictors input into the model, regardless of correlation.

Table 1: The estimate and 95% Confidence Intervals (CI) for $\alpha_{1,\tau}$ and $\alpha_{2,\tau}$ at different quantile levels, $\tau = 0.25, 0.50$ and 0.75 , using the convolution-smoothing based locally sparse estimation (CLoSE) method from the soybean dataset of Kansas.

τ	$\alpha_{1,\tau}$		$\alpha_{2,\tau}$	
	Estimate	95% CI	Estimate	95% CI
0.25	19.26	[-94.23, 84.60]	15.19	[13.03, 23.69]
0.50	5.36	[-56.55, 14.34]	16.69	[14.33, 19.42]
0.75	7.23	[-32.79, 28.42]	15.17	[13.22, 18.34]

Table 1 summarizes 95%-confidence intervals for $\alpha_{1,\tau}$ and $\alpha_{2,\tau}$. We observe that for all three quantiles, the proportion of irrigated areas of each county is significant to the annual soybean yield, while the annual precipitation is not significant for any quantiles.

5 Conclusions and Discussion

In this paper, we propose a locally sparse semi-parametric functional quantile model to study the dynamic dependence of scalar response on functional covariates. A convolution-smoothing based locally sparse estimation (CLOSE) method is developed to identify the locally sparse regions of the functional coefficients and estimate the parameters and the functional coefficients on the non-null regions. We also establish the functional version of the oracle property of the functional coefficients and the asymptotic properties of the estimated parameters. The CLOSE method addresses the difficulty in computation by first convolving the quantile loss function with a smoothing kernel. This step smooths out the function and makes it easier to optimize. The CLOSE method has been shown to be effective in estimating the locally sparse semi-parametric functional quantile model in our simulation studies and real applications.

When the data size is large-scale, the computation burden brought by the fSCAD penalty and the selection of several tuning parameters is heavy even if we use the convolution-smoothed quantile loss. Improving the computation efficiency when analyzing large-scale functional data is indeed an important topic worth investigating in future research. One possible approach is to develop new algorithms that can handle large-scale data more efficiently. For example, one could consider using parallel computing techniques or developing distributed algorithms that can run on clusters of computers.

Supplementary Materials

The supplementary document includes the summarized algorithm of the proposed Convolution-smoothing based Locally Sparse Estimation (CLOSE) method, and the required conditions,

the wild bootstrap method, simulation studies and technical proofs of the theorems. The computing scripts for replicating the simulation studies and the real data application are also provided.

Declarations

Conflict of interest The authors have no conflicts of interest to declare.

References

- Alsajri, F. A., Wijewardana, C., Bheemanahalli, R., Irby, J. T., Krutz, J., Golden, B., Reddy, V. R., and Reddy, K. R. (2022). Morpho-physiological, yield, and transgenerational seed germination responses of soybean to temperature. *Frontiers in Plant Science*, 13:839270.
- Chen, K. and Müller, H.-G. (2012). Conditional quantile analysis when covariates are functions, with application to growth data. *Journal of the Royal Statistical Society: Series B (Statistical Methodology)*, 74(1):67–89.
- Cheng, C., Feng, X., Huang, J., and Liu, X. (2022). Regularized projection score estimation of treatment effects in high-dimensional quantile regression. *Statistica Sinica*, 32(1):23–41.
- Fan, J. and Li, R. (2001). Variable selection via nonconcave penalized likelihood and its oracle properties. *Journal of the American Statistical Association*, 96(456):1348–1360.
- Feng, X., He, X., and Hu, J. (2011). Wild bootstrap for quantile regression. *Biometrika*, 98(4):995–999.

- Fernandes, M., Guerre, E., and Horta, E. (2021). Smoothing quantile regressions. *Journal of Business & Economic Statistics*, 39(1):338–357.
- Guan, T., Lin, Z., and Cao, J. (2020). Estimating truncated functional linear models with a nested group bridge approach. *Journal of Computational and Graphical Statistics*, 29(3):620–628.
- He, X., Pan, X., Tan, K. M., and Zhou, W.-X. (2023). Smoothed quantile regression with large-scale inference. *Journal of Econometrics*, 232(2):367–388.
- Huang, J., Ma, S., Xie, H., and Zhang, C.-H. (2009). A group bridge approach for variable selection. *Biometrika*, 96(2):339–355.
- Hunter, D. R. and Li, R. (2005). Variable selection using MM algorithms. *The Annals of Statistics*, 33(4):1617–1642.
- James, G. M., Wang, J., and Zhu, J. (2009). Functional linear regression that is interpretable. *The Annals of Statistics*, 37(5A):2083–2108.
- Kato, K. (2012). Estimation in functional linear quantile regression. *The Annals of Statistics*, 40(6):3108–3136.
- Koenker, R. and Bassett Jr, G. (1978). Regression quantiles. *Econometrica*, 46(1):33–50.
- Lee, E. R., Noh, H., and Park, B. U. (2014). Model selection via bayesian information criterion for quantile regression models. *Journal of the American Statistical Association*, 109(505):216–229.
- Li, Y., Wang, F., Wu, M., and Ma, S. (2022). Integrative functional linear model for genome-wide association studies with multiple traits. *Biostatistics*, 23(2):574–590.

- Lin, Z., Cao, J., Wang, L., and Wang, H. (2017). Locally sparse estimator for functional linear regression models. *Journal of Computational and Graphical Statistics*, 26(2):306–318.
- Ma, H., Li, T., Zhu, H., and Zhu, Z. (2019). Quantile regression for functional partially linear model in ultra-high dimensions. *Computational Statistics & Data Analysis*, 129:135–147.
- Park, J., Ahn, J., and Jeon, Y. (2022). Sparse functional linear discriminant analysis. *Biometrika*, 109(1):209–226.
- Schlenker, W. and Roberts, M. J. (2009). Nonlinear temperature effects indicate severe damages to us crop yields under climate change. *Proceedings of the National Academy of sciences*, 106(37):15594–15598.
- Szczerba, A., Płazek, A., Pastuszak, J., Kopeć, P., Hornyák, M., and Dubert, F. (2021). Effect of low temperature on germination, growth, and seed yield of four soybean (glycine max l.) cultivars. *Agronomy*, 11(4):800.
- Tan, K. M., Wang, L., and Zhou, W.-X. (2022). High-dimensional quantile regression: Convolution smoothing and concave regularization. *Journal of the Royal Statistical Society: Series B (Statistical Methodology)*, 84(1):205–233.
- Tu, C. Y., Park, J., and Wang, H. (2020). Estimation of functional sparsity in nonparametric varying coefficient models for longitudinal data analysis. *Statistica Sinica*, 30(1):439–465.
- Vogel, E., Donat, M. G., Alexander, L. V., Meinshausen, M., Ray, D. K., Karoly, D.,

- Meinshausen, N., and Frieler, K. (2019). The effects of climate extremes on global agricultural yields. *Environmental Research Letters*, 14(5):054010.
- Wang, H. and Kai, B. (2015). Functional sparsity: Global versus local. *Statistica Sinica*, pages 1337–1354.
- Wang, L., Chen, G., and Li, H. (2007). Group scad regression analysis for microarray time course gene expression data. *Bioinformatics*, 23(12):1486–1494.
- Wang, Z., Magnotti, J., Beauchamp, M. S., and Li, M. (2023). Functional group bridge for simultaneous regression and support estimation. *Biometrics*, 79(2):1226–1238.
- Yao, F., Sue-Chee, S., and Wang, F. (2017). Regularized partially functional quantile regression. *Journal of Multivariate Analysis*, 156:39–56.
- Zhou, J., Wang, N.-Y., and Wang, N. (2013). Functional linear model with zero-value coefficient function at sub-regions. *Statistica Sinica*, 23(1):25–50.
- Zou, H. and Li, R. (2008). One-step sparse estimates in nonconcave penalized likelihood models. *The Annals of Statistics*, 36(4):1509–1533.